arXiv:1408.4197v1 [cond-mat.supr-con] 19 Aug 2014

Superconducting Transition Temperatures of up to 47 K from Simultaneous Rare-Earth Element and Antimony Doping of 112-Type $CaFeAs_2$

Kazutaka Kudo[1,2*], Yutaka Kitahama[1], Kazunori Fujimura[1], Tasuku Mizukami[1], Hiromi Ota[3], and Minoru Nohara[1,2†]

[1]*Department of Physics, Okayama University, Okayama 700-8530, Japan*
[2]*Research Center of New Functional Materials for Energy Production, Storage and Transport, Okayama University, Okayama 700-8530, Japan*
[3]*Division of Instrumental Analysis, Department of Instrumental Analysis & Cryogenics, Advanced Science Research Center, Okayama University, Okayama 700-8530, Japan*

The effects of simultaneous Sb doping on the superconductivity of 112-type $Ca_{1-x}RE_xFeAs_2$ (*RE* = La, Ce, Pr, and Nd) were studied through measurements of the magnetization and electrical resistivity. In Sb-free materials, the superconducting transition temperature T_c of the La-doped sample was 35 K, while those of the Pr- and Nd-doped samples were ~10 K; no superconductivity was observed in the Ce-doped sample. Sb doping increased the T_c of all *RE*-doped samples: T_c increased to 47, 43, 43, and 43 K for *RE* = La, Ce, Pr, and Nd, respectively. We also found that the enhanced superconductivity results from the increase in the lattice parameter *b*, which increases the As-Fe-As bond angle to be closer to the ideal tetrahedron value. These observations provide insight for further increasing the T_c of the 112 phase.

The discovery of iron-based superconductors has stimulated the development of novel superconducting materials[1–3] such as *RE*FeAsO (1111 type),[4] $AEFe_2As_2$ (122 type),[5,6] *A*FeAs (111 type),[7] and FeSe (11 type)[8] that contain rare-earth (*RE*), alkali-earth (*AE*), and alkali (*A*) elements, as well as the development of compounds with perovskite- and/or rocksalt-type[9–12] and pyrite-type spacer layers.[13–18] For this class of materials, the maximum superconducting transition temperature T_c is 55 K,[19] and new iron-based superconducting materials will need to be developed to further increase T_c.

To this end, novel 112-type iron arsenides of $Ca_{1-x}La_xFeAs_2$, $Ca_{1-x}Pr_xFeAs_2$, and $Ca_{1-x}RE_xFeAs_2$ (*RE* = Ce, Nd, Sm, Eu, and Gd) reported by Katayama *et al.*,[20] Yakita *et al.*,[21] and Sala *et al.*,[22] respectively, have received considerable attention, and it has been recognized that the *RE* substitution is necessary for stabilizing the 112 phase.[20–22] These compounds crystallize in a monoclinic structure with a space group of $P2_1$ (No. 4)[20] or $P2_1/m$ (No. 11)[21,22] and consist of alternately stacked FeAs and arsenic zigzag bond layers, which are a notable feature. The arsenic zigzag bond layers are considered to be composed of As^- ions with a $4p^4$ configuration as found in $RETAs_2$ (*T* = Ag, Au).[23] Thus, the chemical formula for these compounds can be written as $(Ca^{2+}_{1-x}RE^{3+}_x)(Fe^{2+}As^{3-})As^- \cdot xe^-$ with an excess charge of xe^-/Fe injected into the $Fe^{2+}As^{3-}$ layers. Most 112-type iron arsenides exhibit superconductivity: La-doped compounds show bulk superconductivity at 35 K,[24] while Pr-, Nd-, Sm-, Eu-, and Gd-doped compounds show superconductivity at 10–15 K with a small shielding volume fraction (VF) of 5–20%.[21,22] Ce-doped compounds rarely exhibit superconductivity.[22]

Recently, it was reported that the simultaneous doping of isovalent P or Sb drastically improves the superconductivity in the La-doped 112 phase; T_c increased to 41 and 43 K as a result of 0.5% P and 1% Sb doping, respectively.[24] In this Letter, we report that a large amount of Sb doping further increases the T_c of $Ca_{1-x}La_xFe(As_{1-y}Sb_y)_2$ to 47 K, which is the second highest T_c after 1111-type iron-based superconductors. Moreover, we show that bulk superconductivity at 43, 43, and 43 K is induced by the simultaneous Sb doping of $Ca_{1-x}RE_xFeAs_2$ with *RE* = Ce, Pr, and Nd, respectively, and that an increase in the lattice parameter *b*, which modifies the As-Fe-As bond angle, is important for optimizing the superconductivity in the 112 phase.

Single crystals of $Ca_{1-x}RE_xFe(As_{1-y}Sb_y)_2$ (*RE* = La, Ce, Pr, and Nd) were grown by heating a mixture of Ca, *RE*, FeAs, As, and Sb powders with nominal compositions of $x = 0.10$ and $0.00 \le y \le 0.10$ (grown quantities of the 112 phase drastically decrease for $y \ge 0.20$). A stoichiometric amount of the mixture was then placed in an aluminum crucible and sealed in an evacuated quartz tube. Samples were prepared in a globe box filled with argon gas. The ampules were heated at 700 °C for 3 h, heated to 1100 °C at a rate of 46 °C/h, and then cooled to 1050 °C at a rate of 1.25 °C/h before furnace cooling. The obtained samples were characterized by powder X-ray diffraction (XRD) using a Rigaku RINT-TTR III X-ray diffractometer with CuK_α radiation and by single-crystal XRD using a Rigaku Single Crystal X-ray Structural Analyzer (Varimax with Saturn). $Ca_{1-x}RE_xFe(As_{1-y}Sb_y)_2$ samples were obtained together with a powder mixture of *RE*As, FeAs, $FeAs_2$, and $CaFe_2As_2$. The single crystals of $Ca_{1-x}RE_xFe(As_{1-y}Sb_y)_2$ separated from the

*kudo@science.okayama-u.ac.jp
†nohara@science.okayama-u.ac.jp

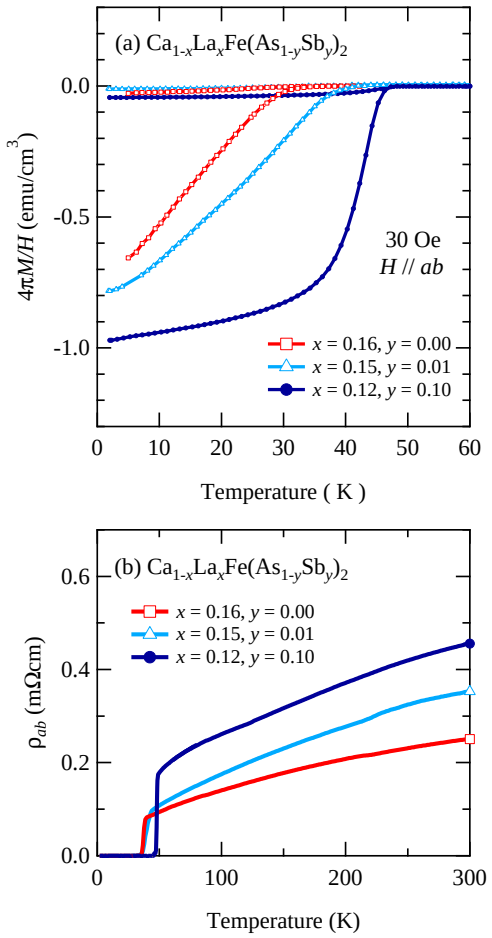

Fig. 1. (Color online) (a) Temperature dependence of the magnetization M of $Ca_{1-x}La_xFe(As_{1-y}Sb_y)_2$ measured at a magnetic field H of 30 Oe parallel to the ab plane under zero-field-cooling and field-cooling conditions. (b) Temperature dependence of the electrical resistivity ρ_{ab} of $Ca_{1-x}La_xFe(As_{1-y}Sb_y)_2$ parallel to the ab plane.

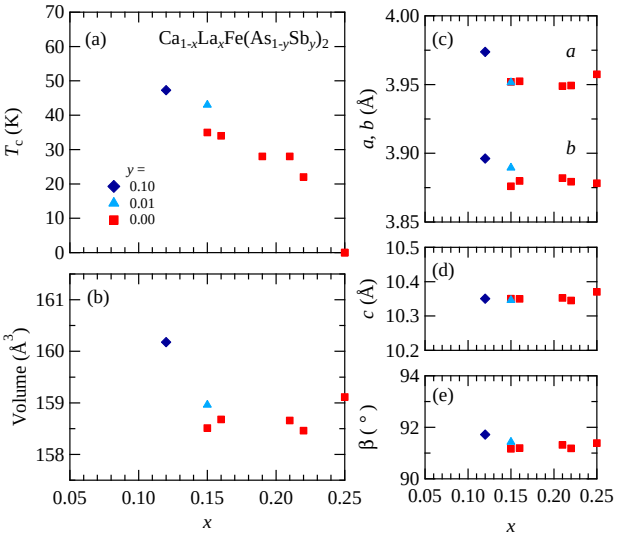

Fig. 2. (Color online) Dependence of the (a) T_c, (b) cell volume, (c) a and b parameters, (d) c parameter, and (e) β angle of $Ca_{1-x}La_xFe(As_{1-y}Sb_y)_2$ on x.

mixture were plate-like with typical dimensions of (0.3–0.7) × (0.3–0.7) × 0.02 mm^3.

The *RE* content x was analyzed by energy-dispersive X-ray spectrometry (EDS), but the Sb content y could not be determined by EDS because the Sb peak positions in the EDS spectra overlapped those of Ca. We thus assumed a nominal y. Although the nominal x was fixed at 0.1, the x values measured by EDS varied with the nominal y. For example, $Ca_{1-x}La_xFe(As_{1-y}Sb_y)_2$ had compositions of x = 0.16, 0.15, and 0.12 with nominal y = 0.00, 0.01, and 0.10, respectively; i.e., the La content tended to decrease with increasing y. In contrast, for $Ca_{1-x}RE_xFeAs_2$ (*RE* = Ce, Pr, and Nd), we found compositions of x = 0.15–0.25 with nominal y = 0.00, 0.01, 0.05, and 0.10; there was no clear relation between x and y.

The magnetization M in a magnetic field of 30 Oe parallel to the ab plane was measured using a Quantum Design magnetic property measurement system (MPMS). The T_c values were determined from the onset of the diamagnetism, which is characteristic of the superconducting transition. Electrical resistivity ρ_{ab} parallel to the ab plane was also measured using a standard DC four-terminal method in a Quantum Design physical property measurement system (PPMS).

The enhancement in the superconductivity of the Sb-doped $Ca_{1-x}La_xFeAs_2$ can be observed in the temperature dependence of M shown in Fig. 1(a). Previous studies[20,24] have reported that La-doped samples with y = 0.00 show diamagnetic behavior below T_c = 34 K,[20] and T_c increased to 43 K for y = 0.01.[24] The values of VF at the lowest temperature were previously estimated to be 66% and 78% for y = 0.00[20] and 0.01,[24] respectively, indicating bulk superconductivity. We found that a large amount of Sb doping leads to a further increase in T_c to 47 K. As shown in Fig. 1(a), the La-doped sample with y = 0.10 exhibits clear diamagnetic behavior below T_c = 47 K, and the VF at 2 K was estimated to be approximately 100%, which supports the emergence of bulk superconductivity. Further evidence of the enhanced superconductivity was obtained from the temperature dependence of ρ_{ab}, as shown in Fig. 1(b). We found that ρ_{ab} for the La-doped y = 0.10 sample exhibited a sharp drop below 49 K, and zero resistivity was observed at 47 K; both these temperatures are much higher than those of the y = 0.00[20] and 0.01[24] samples.

The increased T_c of $Ca_{1-x}La_xFe(As_{1-y}Sb_y)_2$ can be explained by two effects originating from the simultaneous Sb doping: a decrease in the La content and an increase in the cell volume. In $Ca_{1-x}La_xFeAs_2$, it is known that T_c increases with decreasing x and exhibits a maximum value of 35 K at the lowest x of 0.15,[24] as shown in Fig. 2(a); a sample with a lower x could potentially have a higher T_c. Simultaneous Sb

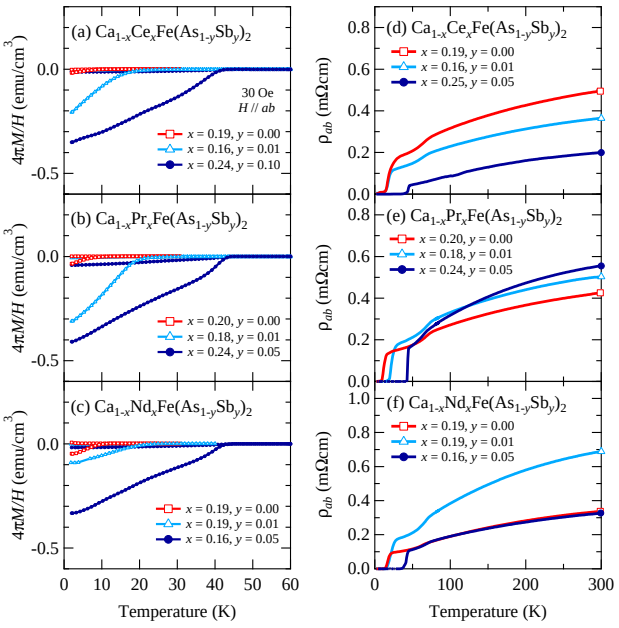
(a) Ca1-xCexFe(As1-ySby)2
30 Oe
H // ab
x = 0.19, y = 0.00
x = 0.16, y = 0.01
x = 0.24, y = 0.10
(b) Ca1-xPrxFe(As1-ySby)2
x = 0.20, y = 0.00
x = 0.18, y = 0.01
x = 0.24, y = 0.05
(c) Ca1-xNdxFe(As1-ySby)2
x = 0.19, y = 0.00
x = 0.19, y = 0.01
x = 0.16, y = 0.05
4πM/H (emu/cm3)
Temperature (K)
(d) Ca1-xCexFe(As1-ySby)2
x = 0.19, y = 0.00
x = 0.16, y = 0.01
x = 0.25, y = 0.05
(e) Ca1-xPrxFe(As1-ySby)2
x = 0.20, y = 0.00
x = 0.18, y = 0.01
x = 0.24, y = 0.05
(f) Ca1-xNdxFe(As1-ySby)2
x = 0.19, y = 0.00
x = 0.19, y = 0.01
x = 0.16, y = 0.05
ρab (mΩcm)
Temperature (K)

Fig. 3. (Color online) (a)(b)(c) Temperature dependence of the magnetization M of $Ca_{1-x}RE_xFe(As_{1-y}Sb_y)_2$ (RE = Ce, Pr, and Nd) measured at a magnetic field H of 30 Oe parallel to the ab plane under zero-field-cooling and field-cooling conditions. (d)(e)(f) Temperature dependence of the electrical resistivity ρ_{ab} of $Ca_{1-x}RE_xFe(As_{1-y}Sb_y)_2$ (RE = Ce, Pr, and Nd) parallel to the ab plane.

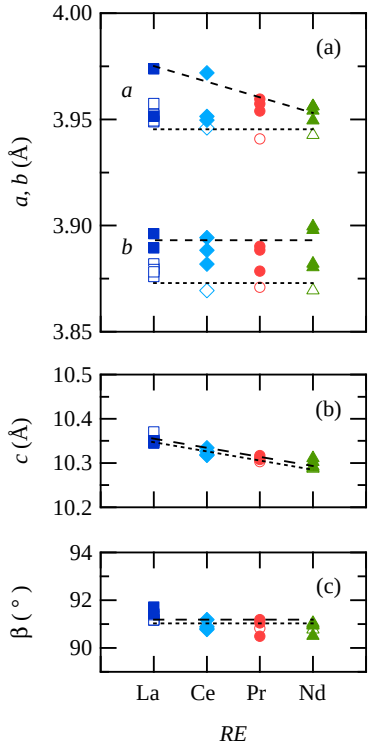

Fig. 4. (Color online) Dependences of the (a) a and b parameters, (b) c parameter, and (c) β angle of $Ca_{1-x}RE_xFe(As_{1-y}Sb_y)_2$ (RE = La, Ce, Pr, and Nd) on RE. The open and closed symbols indicate the lattice parameters of Sb-free samples and Sb-doped samples, respectively. The dotted and broken lines are, respectively, guides to the eye for the lattice parameters of Sb-free samples and Sb-doped samples with the highest T_c for each RE-doped systems.

doping allows the La content to be reduced to $x = 0.12$, and as expected, T_c increased to 47 K. In general, chemical substitution modifies the number of charge carriers and induces a chemical pressure. The primal role of La doping is charge carrier modification because the cell volume [Fig. 2(b)] and lattice parameters[24] [Figs. 2(c), (d), and (e)] of $Ca_{1-x}La_xFeAs_2$ exhibit no significant changes upon La doping owing to the similar ionic radii of Ca^{2+} and La^{3+}. Thus, a decrease in the La content corresponds to a reduction in the number of charge carriers. Secondly, simultaneous Sb doping applies a negative chemical pressure that increases the cell volume, as shown in Fig. 2(b), because the ionic radius of Sb^{3-} (Sb^-) is larger than that of As^{3-} (As^-). The increased cell volume is a result of an increase in the in-plane lattice parameters a and b, as shown in Fig. 2(c); in contrast, the c parameter hardly changes, as shown in Fig. 2(d). In iron-based superconductors, the expansion can effectively optimize the superconductivity, which is sensitive to modifications in the crystal structure.[25–28] Note that the enhancement of T_c by 0.5% P doping in the La-doped system, which was reported in our previous article,[24] should be attributed to a different mechanism because the small amount of P doping[29] neither reduced the La content nor changed the lattice parameters.[24] However, the exact mechanism is still unclear.

A similar enhancement in the superconductivity was also observed in Sb-doped $Ca_{1-x}RE_xFeAs_2$ (RE = Ce, Pr, and Nd). As shown in Figs. 3(a), (b), and (c), in the Sb-free samples, the Ce-doped system shows no bulk superconductivity down to 2 K, while the Pr- and Nd-doped systems exhibit superconductivity at 10 and 11 K, respectively, with a small VF of 5%. These results are consistent with previous reports.[21,22] Sb doping resulted in higher T_c values of 21 and 43 K in Ce-doped systems of $y = 0.01$ and 0.10, respectively, 26 and 43 K in Pr-doped systems of $y = 0.01$ and 0.05, respectively, and 24 and 43 K in Nd-doped systems of $y = 0.01$ and 0.05, respectively. Thus, we found that Sb-doped 112 phase samples have a T_c of higher than 40 K irrespective of RE. More importantly, Sb substitution resulted in a substantial increase in the VF, indicating the emergence of bulk superconductivity. Evidence of the enhanced superconductivity was also found in the temperature dependence of ρ_{ab}. As shown in Figs. 3(d), (e), and (f), ρ_{ab} of $Ca_{1-x}RE_xFe(As_{1-y}Sb_y)_2$ (RE = Ce, Pr, and Nd) with $y = 0.05$ was zero at 37, 43, and 37 K, respectively; these temperatures are much higher than those (5, 9, and 13 K) of the Sb-free samples. Note that the zero resistivity observed in the Sb-free $Ca_{1-x}Ce_xFeAs_2$ sample is attributed to filamentary superconductivity because there is no visible diamagnetic signal at T_c. In $Ca_{1-x}RE_xFe(As_{1-y}Sb_y)_2$ (RE = Ce,

Pr, and Nd), while we have observed the importance of the volume effect [Figs. 4(a) and (b)] in the enhanced superconductivity in the same manner as discussed for the La-doped system, the precise x and y dependences of the T_c are still unclear.

On considering the well-known relation between T_c and local structure in the iron-based superconductors,[25–28] the most important factor that determines the volume effect, which enhances superconductivity, is the increase in the b parameter. In general, iron-based superconductors with high T_c, such as 1111-type superconductors with $T_c > 50$ K, satisfy the following structural conditions: the Fe and As atoms form an ideal tetrahedral structure (i.e., the As-Fe-As bond angle $\alpha = 109.47°$)[25,26] and the As height with respect to the Fe plane, h_{Pn}, is approximately 1.38 Å.[27,28] Because of the monoclinic structure, the 112 phase possesses two bond angles: α_a and α_b, which correspond to the α-angle along the a and b axes, respectively. Our preliminary structural analysis[30] of $Ca_{1-x}La_xFe(As_{1-y}Sb_y)_2$ with $T_c = 47$ K showed that α_b is drastically improved by Sb doping: $\alpha_a = 109.098°$ and $\alpha_b = 107.061°$ in the Sb-free sample,[20] while $\alpha_a = 109.731°$ and $\alpha_b = 108.655°$ in the Sb-doped sample. The result suggests that the increase in b parameter [Fig. 4(a)], which increases α_b, is a key factor for enhancing the superconductivity in the 112 phase.[31] On the other hand, Sb doping does not modify h_{Pn} as much, because the c parameter is almost insensitive to Sb doping [Fig. 4(b)]. In both Sb-free and Sb-doped samples, the h_{Pn} values are slightly larger than the ideal value: $h_{Pn} = 1.418$ and 1.408 Å in the Sb-free[20] and Sb-doped samples, respectively. We expect that the T_c of the 112 phase can be increased above 50 K, if the b parameter can be increased to approximately equal a and, simultaneously, the c parameter can be slightly decreased.

In summary, the effects of Sb doping on the T_c of 112-type $Ca_{1-x}RE_xFeAs_2$ (RE = La, Ce, Pr, and Nd) were studied through measurements of the magnetization and electrical resistivity. Sb-doping results in an increase in T_c such that the T_c values of Sb-doped $Ca_{1-x}RE_xFeAs_2$ with RE = La, Ce, Pr, and Nd were 47, 43, 43, and 43 K, respectively. We found that an increase in the b parameter, which improves the As-Fe-As bond angle, is important for enhancing the superconductivity in the 112 phase.

Acknowledgments This work was partially supported by Grants-in-Aid for Scientific Research (B) (26287082) and (C) (25400372) from the Japan Society for the Promotion of Science (JSPS) and the Funding Program for World-Leading Innovative R&D on Science and Technology (FIRST Program) from JSPS.

1) K. Ishida, Y. Nakai, and H. Hosono, J. Phys. Soc. Jpn. **78**, 062001 (2009).
2) J. Paglione and R. L. Greene, Nat. Phys. **6**, 645 (2010).
3) D. C. Johnston, Adv. Phys. **59**, 803 (2010).
4) Y. Kamihara, T. Watanabe, M. Hirano, and H. Hosono, J. Am. Chem. Soc. **130**, 3296 (2008).
5) M. Rotter, M. Tegel, and D. Johrendt, Phys. Rev. Lett. **101**, 107006 (2008).
6) K. Kudo, K. Iba, M. Takasuga, Y. Kitahama, J. Matsumura, M. Danura, Y. Nogami, and M. Nohara, Sci. Rep. **3**, 1478 (2013).
7) J. H. Tapp, Z. Tang, B. Lv, K. Sasmal, B. Lorenz, P. C. W. Chu, and A. M. Guloy, Phys. Rev. B **78**, 060505(R) (2008).
8) F.-C. Hsu, J.-Y. Luo, K.-W. Yeh, T.-K. Chen, T.-W. Huang, P. M. Wu, Y.-C. Lee, Y.-L. Huang, Y.-Y. Chu, D.-C. Yan, and M.-K. Wu, Proc. Natl. Acad. Sci. U.S.A. **105**, 14262 (2008).
9) N. Kawaguchi, H. Ogino, Y. Shimizu, K. Kishio, and J. Shimoyama, Appl. Phys. Express **3**, 063102 (2010).
10) X. Zhu, F. Han, G. Mu, P. Cheng, B. Shen, B. Zeng, and H.-H. Wen, Phys. Rev. B **79**, 220512(R) (2009).
11) H. Ogino, K. Machida, A. Yamamoto, K. Kishio, J. Shimoyama, T. Tohei, and Y. Ikuhara, Supercond. Sci. Technol. **23**, 115005 (2010).
12) P. M. Shirage, K. Kihou, C.-H. Lee, H. Kito, H. Eisaki, and A. Iyo, Appl. Phys. Lett. **97**, 172506 (2010).
13) S. Kakiya, K. Kudo, Y. Nishikubo, K. Oku, E. Nishibori, H. Sawa, T. Yamamoto, T. Nozaka, and M. Nohara, J. Phys. Soc. Jpn. **80**, 093704 (2011).
14) M. Nohara, S. Kakiya, K. Kudo, Y. Oshiro, S. Araki, T. C. Kobayashi, K. Oku, E. Nishibori, and H. Sawa, Solid State Commun. **152**, 635 (2012).
15) N. Ni, J. M. Allred, B. C. Chan, and R. J. Cava, Proc. Natl. Acad. Sci. **108**, E1019 (2011).
16) C. Löhnert, T. Stürzer, M. Tegel, R. Frankovsky, G. Friederichs, and D. Johrendt, Angew. Chem. Int. Ed. **50**, 9195 (2011).
17) C. Hieke, J. Lippmann, T. Stürzer, G. Friederichs, F. Nitsche, F. Winter, R. Pöttgen, and D. Johrendt, Phil. Mag. **93**, 3680 (2013).
18) K. Kudo, D. Mitsuoka, M. Takasuga, Y. Sugiyama, K. Sugawara, N. Katayama, H. Sawa, H. S. Kubo, K. Takamori, M. Ichioka, T. Fujii, T. Mizokawa, and M. Nohara, Sci. Rep. **3**, 3101 (2013).
19) Z.-A. Ren, W. Lu, J. Yang, W. Yi, X.-L. Shen, Z.-C. Li, G.-C. Che, X.-L. Dong, L.-L. Sun, F. Zhou, and Z.-X. Zhao, Chin. Phys. Lett. **25**, 2215 (2008).
20) N. Katayama, K. Kudo, S. Onari, T. Mizukami, K. Sugawara, Y. Sugiyama, Y. Kitahama, K. Iba, K. Fujimura, N. Nishimoto, M. Nohara, and H. Sawa, J. Phys. Soc. Jpn. **82**, 123702 (2013).
21) H. Yakita, H. Ogino, T. Okada, A. Yamamoto, K. Kishio, T. Tohei, Y. Ikuhara, Y. Gotoh, H. Fujihisa, K. Kataoka, H. Eisaki, and J. Shimoyama, J. Am. Chem. Soc. **136**, 846 (2014).
22) A. Sala, H. Yakita, H. Ogino, T. Okada, A. Yamamoto, K. Kishio, S. Ishida, A. Iyo, H. Eisaki, M. Fujioka, Y. Takano, M. Putti, and J. Shimoyama, Appl. Phys. Express **7**, 073102 (2014).
23) D. Rutzinger, C. Bartsch, M. Doerr, H. Rosner, V. Neu, Th. Doert, and M. Ruck, J. Solid State Chem. **183**, 510 (2010).
24) K. Kudo, T. Mizukami, Y. Kitahama, D. Mitsuoka, K. Iba, K. Fujimura, N. Nishimoto, Y. Hiraoka, and M. Nohara, J. Phys. Soc. Jpn. **83**, 025001 (2014).
25) C.-H. Lee, A. Iyo, H. Eisaki, H. Kito, M. T. Fernandez-Diaz, T. Ito, K. Kihou, H. Matsuhata, M. Braden, and K. Yamada, J. Phys. Soc. Jpn **77**, 083704 (2008).
26) H. Usui and K. Kuroki, Phys. Rev. B **84**, 024505 (2011).
27) K. Kuroki, H. Usui, S. Onari, R. Arita, and H. Aoki, Phys. Rev. B **79**, 224511 (2009).
28) Y. Mizuguchi, Y. Hara, K. Deguchi, S. Tsuda, T. Yamaguchi, K. Takeda, H. Kotegawa, H. Tou, and Y. Takano: Supercond. Sci. Technol. **23**, 054013 (2010).
29) By doping P in a range of more than 1%, the La doped 112 phase was not obtained.
30) The values of α and h_{P_n} were determined on the basis of the crystal structure with the space group $P2_1$ proposed by Katayama *et al.*[20] We have checked that they are nearly unchanged even when using the space group $P2_1/m$ proposed by Yakita *et al.*[21]
31) The increased a parameter [Fig. 4(a)] results in an increased α_a, but the nearly ideal condition of α_a in the Sb-free sample remains almost unchanged in the Sb-doped sample.